THE JOURNAL OF PHYSICAL CHEMISTRY Letters

pubs.acs.org/JPCL Letter

Electronically Excited OH Super-rotors from Water Photodissociation by Using Vacuum Ultraviolet Free-Electron Laser Pulses

Yao Chang,[#] Feng An,[#] Qinming Li,[#] Zijie Luo, Li Che, Jiayue Yang, Zhichao Chen, Weiqing Zhang, Guorong Wu, Xixi Hu,* Daiqian Xie, Kaijun Yuan,* and Xueming Yang

Cite This: *J. Phys. Chem. Lett.* 2020, 11, 7617−7623 Read Online

ACCESS | Metrics & More | Article Recommendations | Supporting Information

ABSTRACT: The fragmentation dynamics of water in a superexcited state play an important role in the ionosphere of the planets and in the photodissociation region (PDR) of the planetary nebula. In this Letter, we experimentally study the fragmentation dynamics of H_2O with the energy above its ionization potential initiated by vacuum ultraviolet free-electron laser pulses. The experimental results indicate that the binary fragmentation channels H + OH and the triple channels O + 2H both present at 96.4 nm photolysis. Electronically excited OH super-rotors (v = 0, $N \geq 36$, or v = 1, $N \geq 34$), with the internal energy just above the OH (A) dissociation energy, are observed for the first time, which are only supported by the large centrifugal barriers. An absolute cross section of these super-rotors is estimated to be $0.7(\pm 0.3) \times 10^{-18}$ cm^2. The tunnelling rates of these extremely rotationally excited states are also analyzed. This work shows a spectacular example of energy transfer from a photon to fragment rotation through photodissociation.

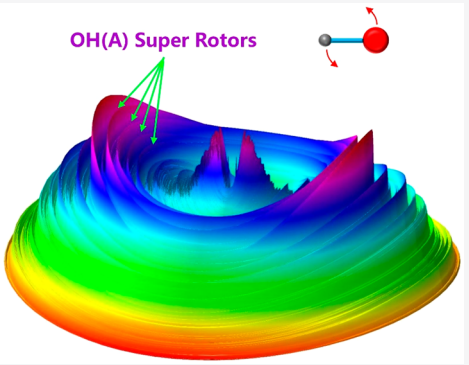

The superexcited molecule, in which a molecule lies in a high Rydberg state with the internal energy higher than its first ionization potential (IP), plays an important role as a reaction intermediate.[1] In particular, these molecules are considered as the Feshbach resonances[2] in the collision between an electron and a molecular ion. The presence of high-energy radiation fields in the universe yields various superexcited molecules. Understanding the fragmentation processes of the superexcited molecule is important in the upper atmosphere of the planets and in the photodissociation region (PDR) of the planetary nebula.[3,4] However, the investigation of such processes is challenging due to the lack of energetic photons in a lab that excite the molecules to the extremely high-lying excited states. With the advent of the intense, pulsed free-electron laser (FEL) in Dalian Coherent Light Source (DCLS) at Dalian, China,[5] the photofragment study of molecules and radicals has become feasible for vacuum-ultraviolet (VUV) wavelengths below 100 nm using the high resolution translational energy spectroscopy.

As a prototype system of molecular fragmentation, the process of $H_2O \rightarrow H + OH$ has been studied extensively, since its importance in the terrestrial atmosphere and in the cometary and planetary atmospheres.[6,7] Excitation around 150−200 nm to the lowest excited singlet state ($\tilde{A}^1B_1$) leads to a direct dissociation that produces an H atom plus OH($X^2\Pi$) with very low internal excitation.[8−12] In contrast, at the Lyman-α wavelength (121.6 nm), the dissociation dynamics are very complicated.[13−15] Direct dissociation following initial excitation to the $\tilde{B}^1A_1$ state yields electronically excited OH($A^2\Sigma^+$) products, together with an H atom. The yield of this adiabatic dissociation channel is relatively minor, however, compared with the major dissociation process yielding ground state OH(X) products via nonadiabatic transitions at the conical intersections (CIs) between the $\tilde{B}$ and $\tilde{X}$ state potential energy surfaces (PESs) at linear H−O−H and H−H−O geometries.[16−21] The high rotational excitations of the OH(X) fragments are generated following this dissociation process and are ascribed to a consequence of strong angular forces at the CI regions.[22−25] A striking odd−even quantum state population alternation of the OH(X, v = 0, N) products has been observed, which was attributed to dynamical quantum interference between pathways that pass through the rival CIs. These studies have deepened our understanding of the peculiar dynamics of H_2O involved. So far, however, limited dissociation dynamics of H_2O on the high-lying potential surfaces are available to benchmark theoretical predictions.

In this Letter, we report the experimental results for photofragmentation of H_2O at 96.4 nm, which excites H_2O to a high Rydberg state lying above its ionization potential

Received: July 29, 2020
Accepted: August 24, 2020
Published: August 24, 2020

https://dx.doi.org/10.1021/acs.jpclett.0c02320
J. Phys. Chem. Lett. 2020, 11, 7617−7623

(IP(H_2O) = 98.2 nm), by using the VUV FEL at DCLS, combined with the H atom Rydberg tagging time-of-flight (HRTOF) technique. The experimental results provide an exotic feature in which electronically excited OH super-rotors, i.e., extremely rotationally excited OH(A) with its internal energy above the bond dissociation limit, are generated. The tunneling lifetimes of these extremely rotationally excited states are investigated.

The experimental arrangement employed in this work represents a newly constructed instrument for molecular photofragmentation around the VUV FEL beamline. The schematic has been shown in Figure 1. The VUV FEL facility

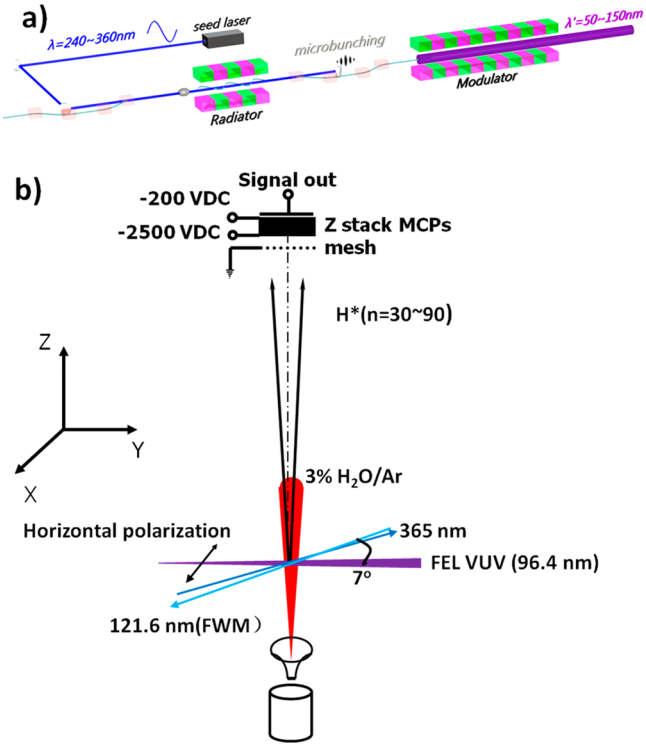

Figure 1. (a) Schematic of the DCLS beam output. (b) Experimental setup for the photodissociation of H_2O by using FEL VUV laser beam. The VUV-FEL facility at the DCLS generates the radiation with the wavelength continuously tuning between 50 and 150 nm. This radiation crosses perpendicularly with the H_2O molecular beam, which is generated by expanding a 3% mixing of H_2O and Ar at a stagnation pressure of 600 Torr through a pulsed nozzle. About 5 ns after the VUV FEL photodissociating H_2O, the H atom products are excited to a high Rydberg state via two-step resonant excitation by absorbing the photons of 121.6 and 365 nm. The neutral Rydberg H atoms then fly a certain TOF distance (~280 mm) to reach a rotatable microchannel plate (MCP) Z-stack detector with a fine metal grid (grounded) in the front and are field-ionized by the electric field (~2500 V/cm) applied between the front plate of the Z-stack MCP detector and the fine metal grid. The signal detected by the MCP is then amplified by a fast preamplifier, and counted by a multichannel scaler.

operates in the High Gain Harmonic Generation mode,[26] in which the seed laser is injected to interact with the electron beam in the modulator. The seeding pulses between 240 and 360 nm are generated by a Ti:sapphire laser. The electron beam generated from a photocathode RF gun is accelerated to the beam energy of ~300 MeV by 7 S-band accelerator structures, with a bunch charge of 500 pC. The microbunched beam is then sent through the radiator, which is tuned to the *n*th harmonic of the seed wavelength, and a coherent FEL pulse at λ/n is emitted. With proper optimization of the linac, a high quality beam with the projected energy spread of ~1‰, and a pulse duration of ~1.5 ps is obtained. The VUV FEL beam pulse operates at 10 Hz, with the photon flux of $\sim 3 \times 10^{14}$/pulse and the wavelength tuning range of 50−150 nm. The spectral bandwidth of the VUV FEL pulses is around 50 cm^{-1}.

The HRTOF technique employs a sequential two-step excitation of the H atom.[27−30] The first step involves the excitation of the H atom from the $n = 1$ ground state to the $n = 2$ state by absorbing one photon at 121.6 nm. The second step concerns the UV laser excitation (365 nm) of the H atom to a high-*n* Rydberg state from the $n = 2$ state. Coherent light source at 121.6 nm is generated by difference four-wave mixing (FWM) of two 212.55 nm photons and one 845 nm photon in a stainless steel cell filled with a 3:1 ratio Ar/Kr mixture. Laser light at 212.55 nm (~1.0 mJ/pulse, and ~0.1 cm^{-1} bandwidth) is produced by doubling the output of a 355 nm (Nd:YAG laser, 8−10 ns) pumped dye laser (Sirah, PESC-G-24) operating at ~425 nm. A portion of the 532 nm output of the same Nd:YAG laser is used to pump another dye laser (Continuum ND6000), which operates at ~845 nm (~5.0 mJ/pulse, and ~0.05 cm^{-1} bandwidth). The remaining 532 nm power from the YAG laser is used to pump a third dye laser (Radiant Dye Laser-Jaguar, D90MA), operating around 732 nm and then doubling to 365 nm (~5.0 mJ/pulse, and ~0.1 cm^{-1} bandwidth). Any charged species formed in the detecting region by multiphoton ionization or autoionization are extracted away from the TOF axis by a small electric field (~30 V/cm) placed across the interaction region. The neutral Rydberg H atoms then fly about 280 mm to reach a rotatable MCP detector and are ionized by the strong electric field (2500 V/cm). The HRTOF technique eliminates the TOF blurring by charged particle interactions, giving a high translational energy resolution of about 0.5%. Since the detection beam of 121.6 nm light would generate photodissociation signals, it is necessary to subtract the 121.6 nm background signal by turning the VUV FEL beam on and off.

H_2O molecules were photoexcited by the VUV FEL radiation to the high Rydberg state through the $nd \leftarrow 1b_1$ transition.[31] At 96.4 nm, only ~30% H_2O molecules were ionized (the H_2O^+ cannot dissociate at this energy), while the rest remained neutral as superexcited molecules.[32] Dissociation on such superexcited state leads to the binary dissociation channels $H_2O \rightarrow H + OH(X/A)$, as well as the triple dissociation channels $H_2O \rightarrow O(^3P/^1D)+2H$. TOF spectra of the H atoms resulting from these channels were then recorded with the detection direction parallel and perpendicular to the laser polarization. Knowing both the distance traveled and the masses of the fragments, the TOF distributions can be transformed into spectra of the total kinetic energy release (E_T(TKER)) by using the equation, $E_T = \frac{1}{2}m_H\left(1 + \frac{m_H}{m_{OH}}\right)\left(\frac{d}{t}\right)^2$, where d is the flying path length of H atom and t is the measured time-of-flight. Photodissociation of HI at 212.5 nm were also performed to calibrate the flying path length.[33] As shown in Figure 2, the E_T spectra display some features that distinguish them from any spectra reported hitherto following H_2O photolysis at longer wavelengths, all of which are dominated by progressions of sharp features, indicating formation of specific rotational quantum states of the OH (X or A) fragments.[19,20] The main feature here is a broad and structureless component in the translational energy region of <~30 000 cm^{-1}. A group of sharp structures are also observed in Figure 2, but are fewer in number. Previous works on H_2O

https://dx.doi.org/10.1021/acs.jpclett.0c02320
J. Phys. Chem. Lett. 2020, 11, 7617−7623

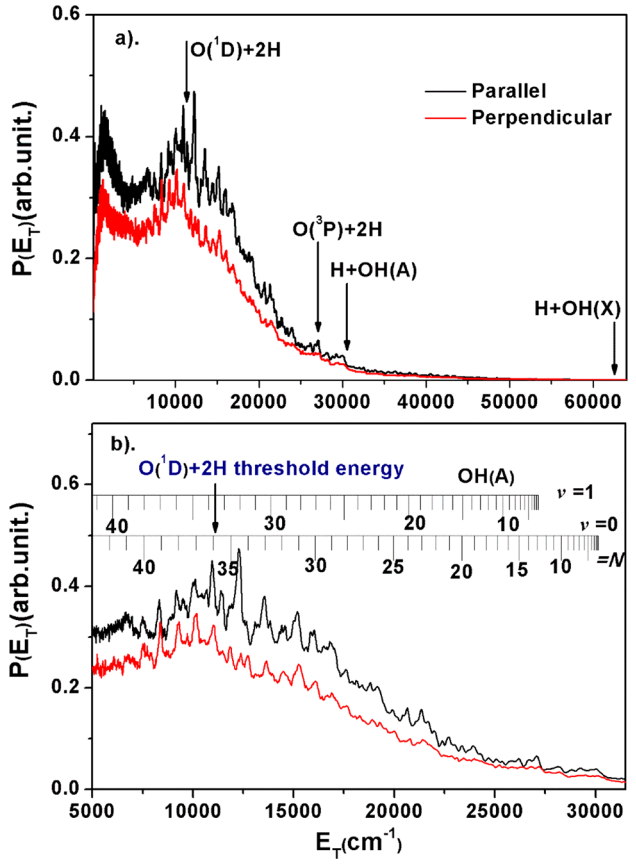

Figure 2. E_T spectra derived from H atom TOF spectra following photodissociation of H_2O at 96.4 nm, with the detection axis parallel (black) or perpendicular (red) to the photolysis laser polarization, ε_{phot}. The energetic limits of the two triple dissociation channels and two binary dissociation channels are marked in (a); the ro-vibrational state assignments are marked in (b).

photodissociation suggested that the E_T spectra of the binary H + OH channel and the triple dissociation channels are characterized by the fine structures and a broad, structureless distribution, respectively.[19,20] Thus, the broad structureless component in Figure 2 should dominantly arise from the triple dissociation channels, whereas the fine structures mainly arise from the binary channels. The overall signal in the parallel direction is a little larger than that in the perpendicular direction, which suggests a parallel transition from the ground state to the high Rydberg state ($nd\ ^1A_1 \leftarrow \tilde{X}^1A_1$). We have also performed a series of experiments in the photolysis wavelengths between 90 and 107 nm, the triple dissociation channels are always dominant, the dynamical features of which are reserved for a future publication. Here we focus on the binary dissociation process.

For the dissociation process, the total energy must be conserved. The internal excitation of the OH fragments (E_{int}(OH)) then is deduced from conservation of momentum and energy,

$$E_{int}(H_2O) + E_{h\nu} - D_0(H{-}OH) = E_{int}(OH) + E_T \quad (1)$$

In the supersonic expansion, the water molecule is cooled down, with a rotational temperature of ~10 K, suggesting $E_{int}(H_2O) \approx 0$. The photon energy, $E_{h\nu}$, and the dissociation energy, D_0(H−OH), are known constants.[19] From eq 1, each peak shown in the E_T spectrum corresponds to a specific rovibrational level of OH. Using previously determined spectroscopy constants for the OH radical,[34] most of the sharp features in the E_T spectra can be then assigned to the OH(A, v', N) (the OH(A, v', N) term values are shown in Table S1 in the Supporting Information). The striking findings in Figure 2B are the formation of extremely rotationally excited OH(A) fragments. The intense peak in the E_T spectra at ~10 860 cm^{-1} involves contributions from the $v' = 0$, $N = 36$, and $v' = 1$, $N = 34$ levels of OH(A), with internal energies above the O(^{1}D) + H dissociation limit.[19] We term such extremely rotationally excited OH products "electronically excited OH super-rotors". The higher energy peak clearly associated with OH(A) can be assigned to $v' = 0$, $N = 40$, or $v'=1$, $N = 38$ fragments, which has an energy of about 0.4 eV above the dissociation limit. Figure 3 shows the OH(X, $v = 0$) rotational

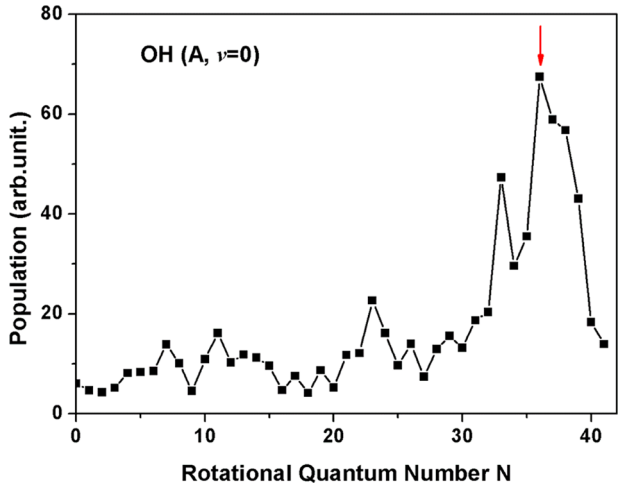

Figure 3. Simulated rotational state population distribution of the OH (A, $v = 0$) products formed in the photodissociation of H_2O at 96.4 nm. The first super-rotor level, above the O (^{1}D) + H dissociation limit, is indicated by the red arrows. The higher super-rotor levels lie to the right of the red arrows.

state population distributions obtained by simulating the E_{int}(OH) spectra (see Figure S1). The level corresponding to the super-rotors is marked by a red arrow. The ground state OH(X) super-rotors have been reported previously by Harich et al.[35] in HOD photodissociation at 121.6 nm, and by Chang et al.[36] in H_2O photodissociation at 115.2 nm. However, the electronically excited OH super-rotors have never been found before, to the best of our knowledge. It is noted that the rotational state distributions are subtly different in the parallel and perpendicular directions (Figure 2), which means the angular distributions are rotational state-specific.

We now seek to gain an explanation for this extremely rotational product distribution. The dissociation mechanism of H_2O in this work is not immediately clear due to the lack of high-lying potential energy surfaces (PESs) of H_2O. It is rational that, however, the OH(A) products are generated via dissociation on the $\tilde{B}$ state PES following internal conversions from the initial excited nd Rydberg states to the $\tilde{B}$ state, since only the $\tilde{B}$ state PES correlates with the H + OH(A) fragments (see Figure S2).[36] The observed rotational energy disposal then relies on the remarkable topography of the $\tilde{B}$ state PES of H_2O. Figure 4 shows a contour plot of the $\tilde{B}$ state PES for one OH bond length fixed at 2.14 bohr, which is equal to the equilibrium bond length of an OH with $v' = 0$, $N = 36$. The surface has deep wells, and the

https://dx.doi.org/10.1021/acs.jpclett.0c02320
J. Phys. Chem. Lett. 2020, 11, 7617−7623

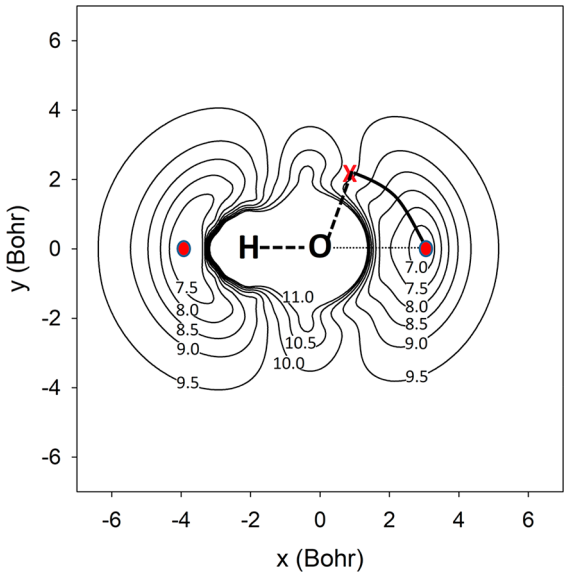

Figure 4. Contour plot of the $\tilde{B}$ state potential energy surface for an OH distance of 2.14 bohr, corresponding to the equilibrium bond length of an OH with $\nu' = 0$, $N = 36$. Energies are given in electronvolts relative to the minimum of the ground state. The initial location of the second H atom is indicated with the red cross. The conical intersections (CIs) at the linear H−O−H and O−H−H geometries, where the minima of the $\tilde{B}$ state PES are degenerate with the maxima of the $\tilde{X}$ state PES, are shown with red dots.

well depths are about 2.5 eV at the two collinear geometries (HOH and HHO). The strong angular anisotropy ensures that the forces point near perpendicular to the radial direction. Thus, the H atom accelerates toward either of the collinear geometries and gains a large amount of orbital angular momentum. At the same time, the OH partner rotates clockwise in order to compensate the change in angular momentum of the H atom, since the total angular momentum must be conserved, i.e., $\mathbf{J} = \mathbf{L} + \mathbf{j}$, where $\mathbf{J}$ is the total angular momentum ($|\mathbf{J}| \approx 0$ in the supersonic beam), $\mathbf{L}$ is the product orbital angular momentum, and $\mathbf{j}$ is the OH rotational angular momentum. The OH(X) fragment then could form on the $\tilde{X}$ state PES via the HOH CI pathway or the OHH CI pathway from the $\tilde{B}$ state to the $\tilde{X}$ state, while the OH(A) product could arise directly on the $\tilde{B}$ state PES, since the H + OH(X) and H + OH(A) channels adiabatically correlate with the $\tilde{X}$ state and the $\tilde{B}$ state PESs, respectively. In both cases, the OH products rotate strongly in order to compensate for the change in angular momentum of the H atom. The extremely high tangential velocities of the departure H atoms ensure the production of the OH super-rotors. The dominant dissociation channel is H + OH(X) from the H_2O photodissociation on the lower electronically excited states, as reported in the previous works.[16−18] In this work, however, the H + OH(X) channel is minor. This suggests that a highly excited H_2O molecule is not necessary to move along the minimum energy path through the two CI pathways of the $\tilde{B}$−$\tilde{X}$ PESs.

The OH super-rotor, with an energy above the bond dissociation limit, only exists by virtue of the associated centrifugal barriers. We have recalculated the potential energy curves (PECs) of OH, as shown in Figure 5. The ground electronic state $X^2\Pi$ and the three repulsive states $a^4\Sigma^-$, $1^2\Sigma^-$, and $1^4\Pi$ asymptotically correlate with the lowest dissociation limit of $O(^3P)$ + H. The $A^2\Sigma^+$ state is correlated to the second dissociation limit of $O(^1D)$ + H. Nuclear rotation has important consequences for the outcome of the dissociation. It modifies the shape of the PECs for the radial Schrödinger equation through centrifugal contributions. The effective potentials for different OH rotational states ($N = 0$, 24, and 42) are shown in Figure 5a−c. For $N = 42$, the barrier is evident. OH formed in these super-rotationally excited levels can dissociate by tunneling through the centrifugal barrier. Figure 5d shows the tunneling lifetimes of these extremely rotationally excited OH levels, calculated using the semiclassical phase integral method.[37] It is interesting to point out that even though the $N = 36$ pure rotational level of OH (A, $\nu = 0$, $N = 36$) is already above its dissociation limit, the tunneling lifetime of this state through the centrifugal barrier is quite long ($>10^{20}$ ps). However, the crossings of the ro-vibrational levels ($\nu = 0$, $N > 24$ or $\nu = 1$, $N > 15$ or $\nu \geq 2$) with the repulsive states ($a^4\Sigma^-$, $1^2\Sigma^-$, and $1^4\Pi$) cause severe predissociation.[38−40] Figure 5e shows the predissociation decay times of some high rotationally excited states of OH (A, $\nu = 0$−5). The predissociation rate is several orders magnitude faster than the tunneling rate. As a result, the lifetimes of the OH (A, $\nu = 0$, $N = 36$−40) super-rotors are around 370−57 ps (a few times of molecular rotation periods). This suggests that these electronically excited super-rotors identified in the present work may have a role in the subsequent chemical reactions in the dense atmosphere. It is interesting to point out that for $N = 24$, the lifetimes of $\nu = 5$ states are longer than lower vibrational states ($\nu = 2$, 3, 4). That is because the $\nu = 2$, 3, 4 states are close to the crossing regions with the three repulsive states, which may have important consequences for predissociation rates.

Through the simulation of the E_T spectra, a branching ratio of the triple dissociation channels and the binary dissociation channels is estimated to be ∼0.8:0.2 (see Figure S1). With the references, the absorption cross-section of H_2O at 96.4 nm is $\sigma_{H_2O} \sim 1.7 \times 10^{-17}$ cm^2, and the ionization quantum yield for H_2O at this wavelength is ∼0.3, suggesting the partial cross section for the neutral H_2O photodissociation would be $\sim 1.7 \times 10^{-17} \times (1 - 0.3) = 1.19 \times 10^{-17}$ cm^2.[32,41] Given the previously reported (small) cross-section for non-H atom forming channels,[42] the absolute cross section for H_2O photodissociation to H + OH(A/X) at 96.4 nm can be estimated to be $1.19 \times 10^{-17} \times 0.2 = \sim(2.4 \pm 1.0) \times 10^{-18}$ cm^2, where the error represents ±10% uncertainty for fitting the triple dissociation channels. Taking 30% OH fragments populating as electronically excited super-rotors, the estimation of the cross-section for forming OH(A) super-rotors at $\lambda = 96.4$ nm: $\sigma \sim (0.7 \pm 0.3) \times 10^{-18}$ cm^2. These highly excited OH fragments are substantially stretched by the centrifugal force. For instance, the mean bond length for $N = 36$ is more than 30% longer than for the rotationless OH molecule, while that of the $N = 40$ is about 45% longer. Since these rotationally excited molecules are significantly stretched like highly vibrationally excited molecules, it would be interesting to compare the physical and chemical properties of these two very different excited species. Thus, the relative large cross section here presents an experimentally feasible way to generate electronically excited OH super-rotors from H_2O photodissociation for substantial investigations. Besides, superexcited H_2O molecules (above the ionization potential), formed by absorbing one VUV photon or colliding between an electron and a molecular ion, might exist in the ionosphere and in the planetary nebula. The neutral fragmentation from these superexcited molecules governs the disappearance of charged species in such circumstances.

https://dx.doi.org/10.1021/acs.jpclett.0c02320
J. Phys. Chem. Lett. 2020, 11, 7617−7623

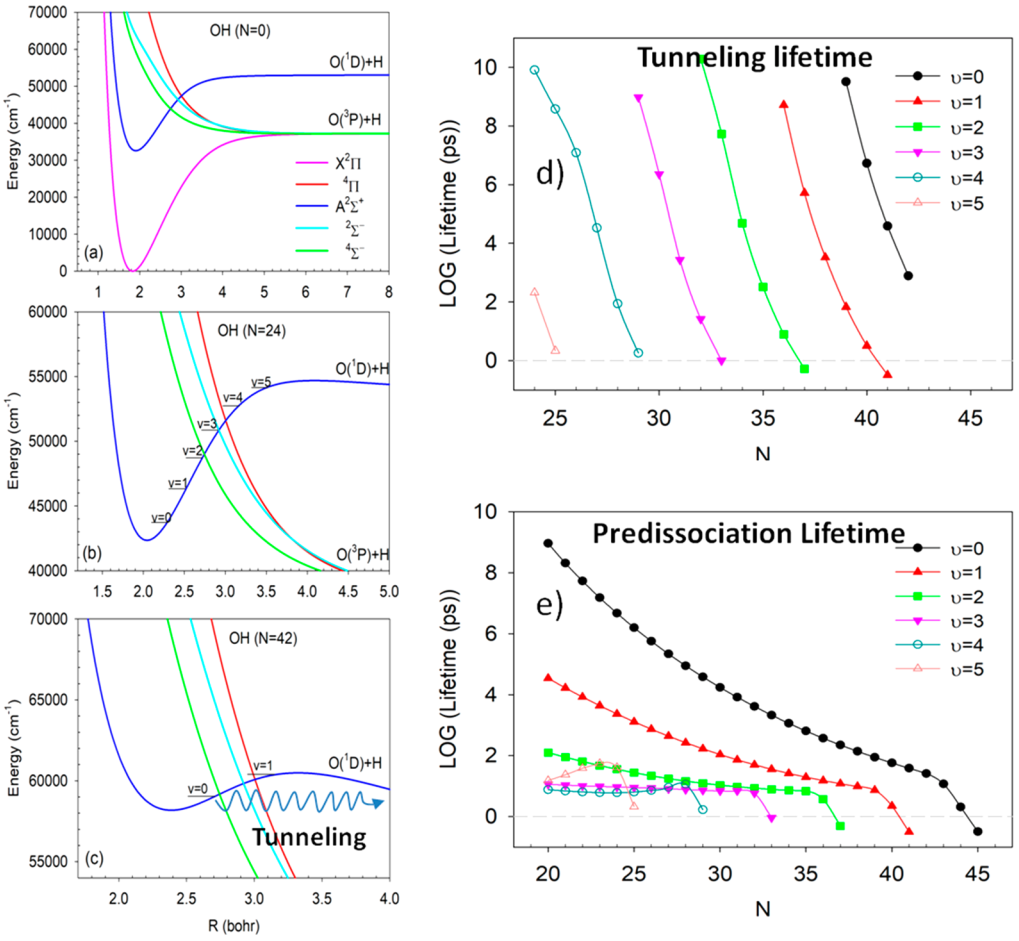

Figure 5. Effective potentials for rotational quantum number N = 0 (a), 24 (b), and 42 (c) as a function of O−H bond length R. The calculated tunneling lifetimes (d) and predissociation lifetimes (e) of high rotationally excited levels of OH ($A^2\Sigma^+$, ν = 0−5).

In summary, we have displayed a benchmark study for photodissociation of the extremely high-lying potential surfaces of H_2O molecules using the new intense VUV free-electron laser. The dominant dissociation channel yields an O atom and two H atoms through the triple dissociation pathways. The extremely rotationally excited OH(A) products are generated in the binary dissociation channels. These dissociation processes may have as yet unrecognized roles in the upper planetary atmosphere.

■ ASSOCIATED CONTENT

Supporting Information

The Supporting Information is available free of charge at https://pubs.acs.org/doi/10.1021/acs.jpclett.0c02320.

Discussion of the dissociation channels, deconvolutions of the E_T spectra, E_T values, energy level diagram, computational details, dissociation energy, excitation energy and equilibrium bond length, and the SO Hamiltonian (PDF)

■ AUTHOR INFORMATION

Corresponding Authors

Xixi Hu − *Key Laboratory of Mesoscopic Chemistry, School of Chemistry and Chemical Engineering, Institute of Theoretical and Computational Chemistry, Nanjing University, Nanjing 210093, China;* orcid.org/0000-0003-1530-3015; Email: xxhu@nju.edu.cn

Kaijun Yuan − *State Key Laboratory of Molecular Reaction Dynamics, Dalian Institute of Chemical Physics, Dalian 116023, China; University of Chinese Academy of Sciences, Beijing 100049, P. R. China;* orcid.org/0000-0002-5108-8984; Email: kjyuan@dicp.ac.cn

Authors

Yao Chang − *State Key Laboratory of Molecular Reaction Dynamics, Dalian Institute of Chemical Physics, Dalian 116023, China*

Feng An − *Key Laboratory of Mesoscopic Chemistry, School of Chemistry and Chemical Engineering, Institute of Theoretical and Computational Chemistry, Nanjing University, Nanjing 210093, China*

Qinming Li − *State Key Laboratory of Molecular Reaction Dynamics, Dalian Institute of Chemical Physics, Dalian 116023, China; University of Chinese Academy of Sciences, Beijing 100049, P. R. China*

Zijie Luo − *State Key Laboratory of Molecular Reaction Dynamics, Dalian Institute of Chemical Physics, Dalian 116023, China; Department of Physics, School of Science, Dalian Maritime University, Dalian, Liaoning 116026, P. R. China*

Li Che − *Department of Physics, School of Science, Dalian Maritime University, Dalian, Liaoning 116026, P. R. China*

Jiayue Yang − *State Key Laboratory of Molecular Reaction Dynamics, Dalian Institute of Chemical Physics, Dalian 116023, China*

https://dx.doi.org/10.1021/acs.jpclett.0c02320
J. Phys. Chem. Lett. 2020, 11, 7617−7623

Zhichao Chen − *State Key Laboratory of Molecular Reaction Dynamics, Dalian Institute of Chemical Physics, Dalian 116023, China*

Weiqing Zhang − *State Key Laboratory of Molecular Reaction Dynamics, Dalian Institute of Chemical Physics, Dalian 116023, China*

Guorong Wu − *State Key Laboratory of Molecular Reaction Dynamics, Dalian Institute of Chemical Physics, Dalian 116023, China;* orcid.org/0000-0002-0212-183X

Daiqian Xie − *Key Laboratory of Mesoscopic Chemistry, School of Chemistry and Chemical Engineering, Institute of Theoretical and Computational Chemistry, Nanjing University, Nanjing 210093, China;* orcid.org/0000-0001-7185-7085

Xueming Yang − *State Key Laboratory of Molecular Reaction Dynamics, Dalian Institute of Chemical Physics, Dalian 116023, China; Department of Chemistry, Southern University of Science and Technology, Shenzhen 518055, China;* orcid.org/0000-0001-6684-9187

Complete contact information is available at: https://pubs.acs.org/10.1021/acs.jpclett.0c02320

Author Contributions

#Y.C., F.A., and Q.L. have equal contributions

Notes

The authors declare no competing financial interest.

■ ACKNOWLEDGMENTS

The experimental work is supported by the National Natural Science Foundation of China (NSFC Nos. 21922306, 21873099, 21673232), the Strategic Priority Research Program of the Chinese Academy of Sciences (Grant No. XDB 17000000), the Chemical Dynamics Research Center (Grant No. 21688102), the international partnership program of Chinese Academy of Sciences (No. 121421KYSB20170012), and the Key Technology Team of the Chinese Academy of Sciences (Grant No. GJJSTD20190002). The theoretical work is supported by NSFC (Nos. 21733006 and 21590802).

■ REFERENCES

(1) Hiraoka, K. In *Fundamentals of Mass Spectrometry*; Hiraoka, K., Ed.; Springer: New York, 2013; Chapter 5.

(2) McDaniel, E. W. *Atomic Collisions Electron and Photon Projectiles*; Wiley Interscience: New York, 1989.

(3) Dabrowski, I.; Herzberg, G. The predicted infrared spectrum of HeH^+ and its possible astrophysical importance. *Trans. N. Y. Acad. Sci.* **1977**, *38*, 14−25.

(4) Black, J. H. Molecules in planetary nebulae. *Astrophys. J.* **1978**, *222*, 125−131.

(5) Chang, Y.; Yu, S.; Li, Q.; Yu, Y.; Wang, H.; Su, S.; Chen, Z.; Che, L.; Wang, X.; Zhang, W.; Dai, D.; Wu, G.; Yuan, K.; Yang, X. Tunable VUV photochemistry using vacuum ultraviolet free electron laser combined with H-atom Rydberg tagging time-of-flight spectroscopy. *Rev. Sci. Instrum.* **2018**, *89*, 063113.

(6) Tappe, A.; Lada, C. J.; Black, J. H.; Muench, A. A. Discovery of Superthermal Hydroxyl (OH) in the HH 211 Outflow. *Astrophys. J.* **2008**, *680*, L117−L120.

(7) Neufeld, D. A.; Dalgarno, A. Fast molecular shocks. I. Reformation of molecules behind a dissociative shock. *Astrophys. J.* **1989**, *340*, 869−893.

(8) Yang, X. F.; Hwang, D. W.; Lin, J. J.; Ying, X. Dissociation dynamics of the water molecule on the $\tilde{A}\ ^1B_1$ electronic surface. *J. Chem. Phys.* **2000**, *113*, 10597−10604.

(9) van Harrevelt, Rob; Hemert, M. C. v. Photodissociation of water in the $\tilde{A}$ band revisited with new potential energy surfaces. *J. Chem. Phys.* **2001**, *114*, 9453−9462.

(10) Zhou, L.; Xie, D.; Sun, Z.; Guo, H. Product fine-structure resolved photodissociation dynamics: the $\tilde{A}$ band of H_2O. *J. Chem. Phys.* **2014**, *140*, 024310.

(11) Lu, I. C.; Wang, F.; Yuan, K.; Cheng, Y.; Yang, X. Nonstatistical spin dynamics in photodissociation of H_2O at 157 nm. *J. Chem. Phys.* **2008**, *128*, 066101.

(12) Schinke, R.; Vander Wal, R. L.; Scott, J. L.; Crim, F. F. The effect of bending vibrations on product rotations in the fully state-resolved photodissociation of the $\tilde{A}$ state of water. *J. Chem. Phys.* **1991**, *94*, 283−288.

(13) von Dirke, Michael; Heumann, Bernd; Kühl, Klaus; Schröder, Thomas; Schinke, R. Fluctuations in absorption spectra and final product state distributions following photodissociation processes. *J. Chem. Phys.* **1994**, *101*, 2051−2068.

(14) van Harrevelt, R.; van Hemert, M. C. Photodissociation of water. I. Electronic structure calculations for the excited states. *J. Chem. Phys.* **2000**, *112*, 5777−5786.

(15) Zhou, L.; Jiang, B.; Xie, D.; Guo, H. State-to-state photodissociation dynamics of H_2O in the B-band: competition between two coexisting nonadiabatic pathways. *J. Phys. Chem. A* **2013**, *117*, 6940−6947.

(16) Mordaunt, D. H.; Ashfold, M. N. R.; Dixon, R. N. Dissociation dynamics of $H_2O(D_2O)$ following photoexcitation at the Lyman-α wavelength (121.6 nm). *J. Chem. Phys.* **1994**, *100*, 7360−7375.

(17) Jiang, B.; Xie, D.; Guo, H. State-to-state photodissociation dynamics of triatomic molecules: H_2O in the B band. *J. Chem. Phys.* **2012**, *136*, 034302.

(18) Dixon, R. N.; Hwang, D. W.; Yang, X. F.; Harich, S.; Lin, J. J.; Yang, X. Chemical "Double Slits": dynamical interference of photodissociation pathways in water. *Science* **1999**, *285*, 1249−53.

(19) Harich, S. A.; Hwang, D. W. H.; Yang, X.; Lin, J. J.; Yang, X.; Dixon, R. N. Photodissociation of H_2O at 121.6 nm: A state-to-state dynamical picture. *J. Chem. Phys.* **2000**, *113*, 10073−10090.

(20) Yuan, K. J.; Dixon, R. N.; Yang, X. M. Photochemistry of the Water Molecule: Adiabatic versus Nonadiabatic Dynamics. *Acc. Chem. Res.* **2011**, *44*, 369−378.

(21) Harich, S. A.; Yang, X. F.; Yang, X.; van Harrevelt, R.; van Hemert, M. C. Single rotational product propensity in the photodissociation of HOD. *Phys. Rev. Lett.* **2001**, *87*, 263001.

(22) He, Z.; Yang, D.; Chen, Z.; Yuan, K.; Dai, D.; Wu, G.; Yang, X. An accidental resonance mediated predissociation pathway of water molecules excited to the electronic C[combining tilde] state. *Phys. Chem. Chem. Phys.* **2017**, *19*, 29795−29800.

(23) Yuan, K.; Cheng, L.; Cheng, Y.; Guo, Q.; Dai, D.; Yang, X. Two-photon photodissociation dynamics of H_2O via the D ∼ electronic state. *J. Chem. Phys.* **2009**, *131*, 074301.

(24) Yuan, K.; Cheng, Y.; Cheng, L.; Guo, Q.; Dai, D.; Wang, X.; Yang, X.; Dixon, R. N. Nonadiabatic dissociation dynamics in H_2O: Competition between rotationally and nonrotationally mediated pathways. *Proc. Natl. Acad. Sci. U. S. A.* **2008**, *105*, 19148−19153.

(25) Wang, H.; Yu, Y.; Chang, Y.; Su, S.; Yu, S.; Li, Q.; Tao, K.; Ding, H.; Yang, J.; Wang, G.; Che, L.; He, Z.; Chen, Z.; Wang, X.; Zhang, W.; Dai, D.; Wu, G.; Yuan, K.; Yang, X. Photodissociation dynamics of H_2O at 111.5 nm by a vacuum ultraviolet free electron laser. *J. Chem. Phys.* **2018**, *148*, 124301.

(26) Yu, L.; Babzien, M.; Ben-Zvi, I. I.; DiMauro, L. F.; Doyuran, A.; Graves, W.; Johnson, E.; Krinsky, S.; Malone, R.; Pogorelsky, I. I.; Skaritka, J.; Rakowsky, G.; Solomon, L.; Wang, X. J.; Woodle, M.; Yakimenko, V. V.; Biedron, S. G.; Galayda, J. N.; Gluskin, E.; Jagger, J.; Sajaev, V. V.; Vasserman, I. I. High-gain harmonic-generation free-electron laser. *Science* **2000**, *289*, 932−934.

(27) Schnieder, L.; Meier, W.; Welge, K. H.; Ashfold, M. N. R.; Western, C. M. Photodissociation dynamics of H_2S at 121.6 nm and a determination of the potential energy function of $SH(A\ ^2\Sigma^+)$. *J. Chem. Phys.* **1990**, *92*, 7027−7037.

(28) Chang, Y.; Chen, Z.; Zhou, J.; Luo, Z.; He, Z.; Wu, G.; Ashfold, M. N. R.; Yuan, K.; Yang, X. Striking Isotopologue-Dependent Photodissociation Dynamics of Water Molecules: The Signature of an Accidental Resonance. *J. Phys. Chem. Lett.* **2019**, *10*, 4209−4214.
(29) Zhou, J.; Zhao, Y.; Hansen, C. S.; Yang, J.; Chang, Y.; Yu, Y.; Cheng, G.; Chen, Z.; He, Z.; Yu, S.; Ding, H.; Zhang, W.; Wu, G.; Dai, D.; Western, C. M.; Ashfold, M. N. R.; Yuan, K.; Yang, X. Ultraviolet photolysis of H_2S and its implications for SH radical production in the interstellar medium. *Nat. Commun.* **2020**, *11*, 1547.
(30) Chang, Y.; Yang, J.; Chen, Z.; Zhang, Z.; Yu, Y.; Li, Q.; He, Z.; Zhang, W.; Wu, G.; Ingle, R. A.; Bain, M.; Ashfold, M. N. R.; Yuan, K.; Yang, X.; Hansen, C. S. Ultraviolet photochemistry of ethane: implications for the atmospheric chemistry of the gas giants. *Chem. Sci.* **2020**, *11*, 5089−5097.
(31) Fillion, J. H.; Ruiz, J.; Yang, X. F.; Castillejo, M.; Rostas, F.; Lemaire, J. L. High resolution photoabsorption and photofragment fluorescence spectroscopy of water between 10.9 and 12 eV. *J. Chem. Phys.* **2004**, *120*, 6531−6541.
(32) Fillion, J. H.; Dulieu, F.; Baouche, S.; Lemaire, J. L.; Jochims, H. W.; Leach, S. Ionization yield and absorption spectra reveal superexcited Rydberg state relaxation processes in H_2O and D_2O. *J. Phys. B: At., Mol. Opt. Phys.* **2003**, *36*, 2767−2776.
(33) Langford, S. R.; Regan, P. M.; Orr-Ewing, A. J.; Ashfold, M. N. R. On the UV photodissociation dynamics of hydrogen iodide. *Chem. Phys.* **1998**, *231*, 245−260.
(34) Coxon, J. A. Optimum molecular constants and term values for the $X^2\Pi(v \leq 5)$ and $A^2\Sigma^+(v \leq 3)$ States of OH. *Can. J. Phys.* **1980**, *58*, 933−949.
(35) Harich, S. A.; Yang, X.; Yang, X.; Dixon, R. N. Extremely rotationally excited OH from water (HOD) photodissociation through conical intersection. *Phys. Rev. Lett.* **2001**, *87*, 253201.
(36) Chang, Y.; Yu, Y.; Wang, H.; Hu, X.; Li, Q.; Yang, J.; Su, S.; He, Z.; Chen, Z.; Che, L.; Wang, X.; Zhang, W.; Wu, G.; Xie, D.; Ashfold, M. N. R.; Yuan, K.; Yang, X. Hydroxyl super rotors from vacuum ultraviolet photodissociation of water. *Nat. Commun.* **2019**, *10*, 1250.
(37) Le Roy, R. J.; Liu, W. K. Energies and widths of quasibound levels (orbiting resonances) for spherical potentials. *J. Chem. Phys.* **1978**, *69*, 3622−3631.
(38) Gray, J. A.; Farrow, R. L. Predissociation lifetimes of OH $A\,^2\Sigma^+$ (v′=3) obtained from optical−optical double-resonance linewidth measurements. *J. Chem. Phys.* **1991**, *95*, 7054−7060.
(39) Heard, D. E.; Crosley, D. R.; Jeffries, J. B.; Smith, G. P.; Hirano, A. Rotational level dependence of predissociation in the v′=3 level of OH $A\,^2\Sigma^+$. *J. Chem. Phys.* **1992**, *96*, 4366−4371.
(40) Spaanjaars, J. J. L.; ter Meulen, J. J.; Meijer, G. Relative predissociation rates of OH ($A\,^2\Sigma^+$, v′=3) from combined cavity ring down—Laser-induced fluorescence measurements. *J. Chem. Phys.* **1997**, *107*, 2242−2248.
(41) Lee, L. C.; Suto, M. quantitative photoabsorption and fluorescence study of H_2O and D_2O at 50−190nm. *Chem. Phys.* **1986**, *110*, 161−169.
(42) van Harrevelt, R.; van Hemert, M. C. Quantum mechanical calculations for the $H_2O+h\nu \rightarrow O(^1D)+H_2$ photodissociation process. *J. Phys. Chem. A* **2008**, *112*, 3002−3009.

https://dx.doi.org/10.1021/acs.jpclett.0c02320
J. Phys. Chem. Lett. 2020, 11, 7617−7623